The Electronic Spectrum of Chloroformic Acid in Comparison to Formic Acid

Margret Gruber-Stadler,[†,‡] Max Mühlhäuser,[*,†] and Claus J. Nielsen[‡]

Studiengang Verfahrens- and Umwelttechnik, MCI − Management Center Innsbruck, Internationale Fachhochschulgesellschaft mbH, Egger-Lienz-Strasse 120, A-6020 Innsbruck, Austria, and Department of Chemistry, University of Oslo, Blindern, N-0315 Oslo, Norway

Received: October 19, 2005; In Final Form: March 21, 2006

The electronic spectra of chloroformic acid ClCOOH and formic acid HCOOH are computed in large-scale multireference configuration interaction (MRD-CI) calculations. The computed spectrum of formic acid is in reasonable agreement with prior calculations and experimental data. The first electronic transition of ClCOOH is computed at 6.41 eV (193.4 nm), about 0.5 eV higher than in HCOOH. Together with five strong transitions calculated at 7.66 eV (161.9 nm; $2^1A' \leftarrow X^1A'$), 8.36 eV (148.3 nm; $3^1A' \leftarrow X^1A'$), 8.49 eV (146.0 nm; $4^1A' \leftarrow X^1A'$), 9.00 eV (137.8 nm; $5^1A' \leftarrow X^1A'$), and 9.44 eV (131.3 nm; $7^1A' \leftarrow X^1A'$), this can serve as a guideline for experimental search of ClCOOH.

1. Introduction

Hydrocarbons, chlorine-substituted hydrocarbons, and acids have received large interest in atmospheric chemistry.[1−11] The photoabsorption of HCOOH has been extensively investigated experimentally in both the vacuum UV and the UV region.[12−22] The photodissociation of formic acid in the vapor phase was studied recently,[23−26] and corresponding quantum chemical calculations have been reported.[13,14,17,22,27−29]

Formic and acetic acids are detected in the upper troposphere and in rainwater.[30−33] Although chlorine-substituted hydrocarbons are known to be important reaction intermediates in atmospheric processes, much less is known about the photochemistry of chloroformic acid. West et al.[34] studied the photochemical reaction of chlorine with formic acid to give chloroformic acid as an intermediate. Herr, Pimentel, and Jensen[35−37] examined the unimolecular decomposition of chloroformic acid by rapid-scan infrared spectroscopy. Francisco et al.[38] and Stephenson et al.[39] used ab initio quantum chemical calculations to study the dissociation of ClCOOH on the electronic ground-state potential surface. The electronic absorption spectrum in the UV and vacuum UV region has not been published yet. On the other hand, a study of excited states of ClCOOH can help to clarify its role as a possible reaction intermediate in atmospheric processes as proposed by Francisco et al.[38] and Jensen et al.[37]

Quantum chemical calculations are an almost ideal tool to investigate excited states and to characterize short-lived intermediates. Such an endeavor requires first the calculation of many electronically excited states and the probability for populating these states. Multireference configuration procedures are required for a balanced description of such states. The computation of potential energy surfaces of excited states and structures far from equilibrium requires multireference methods. Such MRD-CI calculations have recently been very successful for various halocarbons.[8−10] Therefore, in the present study we performed large-scale multireference configuration interaction MRD-CI calculations of electronically excited states and the probability of populating these states to predict the electronic spectrum of chloroformic acid.

After a brief summary describing the computational techniques used in section 2, we will present in section 3 the results obtained and discuss the electronic spectrum of ClCOOH in comparison to formic acid HCOOH, a species that has been well examined theoretically[13,14,17,22,27−29] and experimentally.[12−26] Finally, in section 4 some important conclusions will be summarized.

2. Computational Techniques

The equilibrium geometries of formic acid and chloroformic acid are well established from experimental and theoretical studies.[22,38−41] For practical reasons, however, the present calculations of excited states are based on equilibrium geometries, which we determined employing density functional methods (BP86[42]) and the TURBOMOLE program package V5-4.[43] As discussed below, the equilibrium geometries we used are in reasonable agreement with the values reported in the literature.

For the calculation of excited states, we examined several different basis sets. For the computation of formic acid, we used a correlation consistent atomic orbital (AO) basis set of triple-ζ quality[44] cc-pVTZ+SPD augmented by s-, p-, and d-Rydberg functions located at the carbon and oxygen centers. The exponents taken are $\alpha_s(C) = 0.023$, $\alpha_p(C) = 0.021$, $\alpha_d(C) = 0.015$, $\alpha_s(O) = 0.032$, $\alpha_p(O) = 0.028$, and $\alpha_d(O) = 0.015$.[45] With this cc-pVTZ+SPD basis set, we computed 8 roots per irreducible representation (IRREP) for all singlet states. In addition, we performed calculations employing a smaller polarized cc-pVDZ+SPD basis set of double-ζ quality,[46] enlarged by the same s-, p-, and d-Rydberg functions as stated above for the cc-pVTZ+SPD basis set. As can be seen from Table 1, there are only minor changes in excitation energies and in the transition probabilities when using this more economic cc-pVDZ+SPD basis set. Therefore, we calculated 8 roots per IRREP of all singlet and triplet excited states of formic acid and chloroformic acid, employing the more economic cc-pVDZ+SPD basis set because we furthermore find that it is

* Corresponding author. E-mail: max.muehlhaeuser@mci.edu.
† MCI − Management Center Innsbruck.
‡ University of Oslo.

10.1021/jp0559938 CCC: $33.50
Published on Web 04/18/2006

TABLE 1: Calculated Electronic Transition Energies ΔE (eV and nm) and Oscillator Strengths f from the Ground-State X^1A' of HCOOH to Its Electronically Excited Singlet (ΔE(sing)) and Triplet (ΔE(trip)) States[a]

		ΔE(sing)[b]		ΔE(sing)[c]			ΔE(trip)[c]	ΔE(exptl.)		ΔE(calc)	
state	excitation	[eV]	f[b]	[eV]	[nm]	f[c]	[eV]	[eV]	[nm]	[eV]	[nm]
X^1A'	$(7a')^2(2a'')^2$	0.00		0.00							
$1A''$	$7a' \rightarrow 3a''$	5.96	0.003	5.88	210.9	0.002	5.62	4.64[22]	267.2	5.24[29]	236.6
								5.7[13]	217.5	5.80[28]	213.8
								5.8[15]	213.8	5.83[27]	212.7
										6.0[13]	206.6
										6.86[14]	180.7
$2A'$	$7a' \rightarrow 8a'$	8.08	0.006	7.80	159.0	0.004	7.85	7.5[12]	165.3	8.14[29]	152.3
								7.6[13]	163.1		
								7.7[15]	161.0		
								8.1[16]	153.1		
$3A'$	$7a' \rightarrow 9a'$	8.76	0.06	8.44	146.9	0.06	8.50	8.84[12]	140.3	9.16[29]	135.4
								8.95[16]	138.5		
$4A'$	$2a'' \rightarrow 3a''$	8.83	0.2	8.83	140.4	0.2	6.50	8.107[12]	152.9	8.9[13]	139.3
								8.4[13,15]	147.6	9.52[28]	130.2
										9.64[29]	128.6
										9.84[27]	126.0
										12.02[14]	103.1
$2A''$	$7a' \rightarrow 4a''$	9.39	0.002	8.99	137.9	0.0003	9.01	8.84[16]	140.3	9.15[29]	135.5
								8.9[15]	139.3		

[a] The excitation energies are given with respect to the ground-state configuration $(7a')^2(2a'')^2$ (valence electrons only). The results using the cc-pVDZ+SPD and the cc-pVTZ+SPD (s-, p-, and d-Rydberg functions located at all heavy atoms) basis sets are compared. All values are obtained at the MRD-CI+Q level as explained in the Computational Techniques. [b] cc-pVTZ+SPD basis set, this work. [c] cc-pVDZ+SPD basis set, this work.

TABLE 2: Calculated Electronic Transition Energies ΔE (eV and nm) and Oscillator Strengths f from the Ground-State X^1A' of ClCOOH to Its Electronically Excited Singlet (ΔE(sing)) and Triplet (ΔE(trip)) States[a]

		ΔE(sing)[b]		ΔE(sing)[c]			ΔE(trip)[c]
state	excitation	[eV]	[nm]	[eV]	[nm]	f[c]	[eV]
X^1A'	$(9a')^2(3a'')^2$	0.00		0.00			
$1A''$	$9a' \rightarrow 4a''$	6.33	195.9	6.41	193.4	0.0007	6.19
$2A'$	$9a' \rightarrow 10a'$	7.78	159.4	7.66	161.9	0.03	7.28
$3A'$	$3a'' \rightarrow 4a''$	8.39	147.8	8.36	148.3	0.1	7.94
$2A''$	$3a'' \rightarrow 10a'$	8.37	148.1	8.29	149.6	0.0003	7.80
$3A''$	$8a' \rightarrow 4a''$	8.37	148.1	8.38	148.0	0.013	8.35
$4A'$	$8a' \rightarrow 10a'$	8.42	147.2	8.49	146.0	0.1	8.18
$5A'$	$9a' \rightarrow 11a'$ ($8a' \rightarrow 10a'$)			9.00	137.8	0.06	9.01
$4A''$	$2a'' \rightarrow 10a'$	8.85	140.1	9.25	134.0	0.0002	8.65
$6A'$	$3a'' \rightarrow 11a'$ ($2a'' \rightarrow 10a'$)			9.30	133.3	0.0002	8.83
$7A'$	$2a'' \rightarrow 4a''$	8.98	138.1			0.28[b]	6.85
$8A'$	$9a' \rightarrow 12a'$ ($8a' \rightarrow 10a'$)			9.44	131.3	0.12	

[a] The excitation energies are given with respect to the ground-state configuration $(9a')^2(3a'')^2$ (valence electrons only). For comparison, the results of calculations using the cc-pVDZ and the cc-pVDZ+SPD (s-, p-, and d-Rydberg functions located at all heavy atoms) basis sets are presented. All values are obtained at the MRD-CI+Q level as explained in the Computational Techniques. [b] cc-pVDZ basis set. [c] cc-pVDZ+SPD basis set.

very important to compute at least 8 roots to obtain the correct ordering of states. For the calculations of excited states of ClCOOH, the corresponding s-, p-, and d-Rydberg functions for chlorine are $\alpha_s(Cl) = 0.025$, $\alpha_p(Cl) = 0.020$, and $\alpha_d(Cl) = 0.015$.[45] The values obtained for formic acid are in reasonable agreement with both the results of other computations and the experimental findings as can be seen from Table 1.

Additionally we computed excited states of formic acid and chloroformic acid employing cc-pVDZ[46] basis sets without any Rydberg functions. For the calculation of formic acid, the inclusion of Rydberg functions is very important, whereas the results in the lower energy range up to 8.5 eV obtained for chloroformic acid are much less affected by the employment of Rydberg functions as can be seen from Table 2.

The cc-pVDZ+SPD basis set is flexible with respect to polarization and electron correlation and is considered to be fairly balanced for all states treated so that calculated transition energies are expected to be within an error margin of 0.3 eV.

The computations of the electronically excited states were performed with the selecting multireference single- and double-excitation configuration interaction method MRD-CI implemented in the DIESEL program.[47] The selection of reference configurations can be carried out automatically according to a summation threshold. We have chosen a summation threshold of 0.85, which means that the sum of the squared coefficients of all reference configurations selected for each electronic state (root) is above 0.85. The number of reference configurations for each irreducible representation was in the range between 11 and 21 for HCOOH and between 28 and 41 for ClCOOH. An analysis of the molecular orbitals (MO) involved in the selected reference configurations justifies our prior choice of treating the 18 valence electrons (HCOOH) and 25 valence electrons (ClCOOH) active while keeping the remaining electrons in doubly occupied orbitals (frozen).

From this set of reference configurations (mains), all single and double excitations in the form of configuration state functions (CSFs) are generated. From this MRD-CI space, all configurations with an energy contribution $\Delta E(T)$ above a given threshold T were selected; that is, the contribution of a configuration larger than this value relative to the energy of

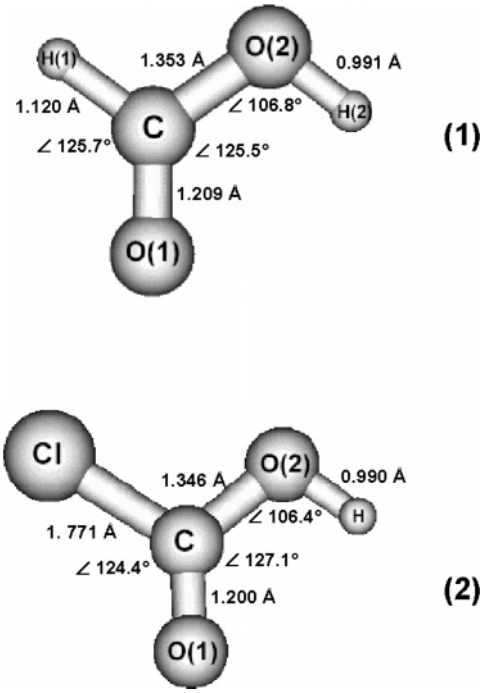

Figure 1. Equilibrium geometry of formic acid HCOOH (1) and chloroformic acid ClCOOH (2) obtained with BP86/cc-pVTZ[42,43] optimizations as explained in the text.

the reference set is included in the final wave function. A selection threshold of $T = 10^{-7}$ hartree and $T = 5 \times 10^{-8}$ hartree was used for the calculation of the excited states of formic acid and chloroformic acid, respectively. The effect of those configurations that contribute less than $T = 10^{-7}$ hartree and $T = 5 \times 10^{-8}$ hartree, respectively, is accounted for in the energy computation (E(MRD-CI)) by a perturbative technique.[48,49] The contribution of higher excitations is estimated by applying a generalized Langhoff−Davidson correction formula E(MRD-CI + Q) = E(MRD-CI) − $(1 - c_0^2)[E(\text{ref}) - E(\text{MRD-CI})]/c_0^2$, where c_0^2 is the sum of squared coefficients of the reference species in the total CI wave function and E(ref) is the energy of the reference configurations.

In total, we examined 32 low-lying electronically excited states (the lowest 16 singlet and the lowest 16 triplet states) of formic acid and 25 low-lying electronically excited states (the lowest 16 singlet and lowest 9 triplet states) of chloroformic acid. The number of configuration state functions (CSFs) directly included in the energy calculations of formic acid is as large as 890000 (singlet) and 760000 (triplet) selected from a total space of 3.9 million (singlet) and 6.7 million (triplet) generated CSFs. For chloroformic acid, 3.35 million (singlet) and 3.25 million (triplet) were selected from a total space of 12.9 million (singlet) and 22.0 million (triplet) generated configurations.

3. Results and Discussion

The equilibrium geometries employed in the present study of excited states are shown in Figure 1 (formic acid (1) and chloroformic acid (2)). It is well known that the ground states of both acids are planar with C_s symmetry.[22,38−41] Both ground states correspond to the isomers with O═C−O−H cis (or syn-planar) configuration. For HCOOH, it can be seen from Figure 1 that the equilibrium geometry we used for our further investigation is in reasonable agreement (deviations of less than 0.04 Å for bond lengths and less than 2° for angles) with the values reported in the literature.[22,40,41] The equilibrium geometry of ClCOOH presently used also agrees well (bond length deviations < 0.025 Å, angles < 1.5°) with the results reported by Francisco et al.,[38] Stephenson et al.,[39] and Remko[41] who computed the equilibrium geometry of ClCOOH at the MP2 level of theory.

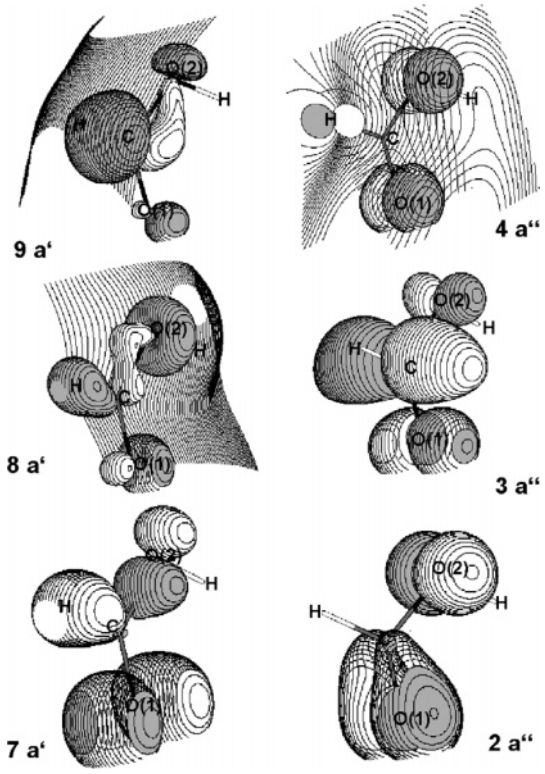

Figure 2. Charge density contours of characteristic occupied (7a′, 2a″) and virtual orbitals (8a′, 9a′, 3a″, and 4a″) of formic acid HCOOH.

3.1. Spectrum of Formic Acid. In Table 1, we compare our presently computed electronic spectrum of formic acid with several experimental and theoretical values from the literature.[12−16,22,27−29] In addition, we compare the results of cc-pVTZ+SPD and cc-pVDZ+SPD basis sets. It can be seen that both results are in reasonable agreement with prior experimental and theoretical findings. In the following, we will give a brief summary of the important features of the electronic spectrum of HCOOH.

The ground state of this molecule is a singlet state X^1A' with the electronic configuration $(7a')^2(2a'')^2$ (valence electrons only). Excitations out of the highest occupied molecular orbital HOMO 7a′ as well as out of the valence orbital 2a″ into the low-lying virtual orbitals 3a″ (LUMO), 8a′, 9a′, and 4a″ are known to be important for the description of the spectrum. In Figure 2, we present charge density contours of important occupied (7a′ and 2a″) and virtual (3a″, 4a″, 8a′, and 9a′) molecular orbitals.

The lowest energy singlet−singlet valence transition (HOMO−LUMO) 7a′ → 3a″ is presently computed at 5.88 eV (210.9 nm). As can be seen from Figure 2, the transition corresponds to a weak ($f = 0.002$) $n_{O(1)} \rightarrow \pi^*_{OCO}$ and $n_{O(2)} \rightarrow \pi^*_{OCO}$-type transition of the O═C−O framework. Prior computations (see Table 1) place this excitation between 5.24 eV (Demoulin et al.;[29] $f \approx 0.014$) and 6.86 eV (Basch et al.;[14] $f \approx 0.007$). Such low-energy UV absorption bands of rather low intensity due to the excitation of nonbonding (n) electrons into antibonding π^* orbitals are well known for organic molecules, which contain oxygen in an unsaturated group.[50] Experimental measurements place the electronic origin of this transition between 4.64 eV (267.2 nm)[22] and 5.8 eV (213.8 nm).[15] The presently computed singlet−triplet splitting of almost 0.3 eV is in line with the value expected for a valence transition.

The next low-lying excitation 7a′ → 8a′ originates from the HOMO (7a′), which is dominated by the nonbonding lone pairs of the two oxygen atoms and a σ-bonding of carbon and hydrogen. The calculated excitation energy of 7.80 eV (159.0 nm) is in good agreement with the experimental measurements reported by Fridh,[13] Ari et al.,[15] and Bell et al.,[16] as well as with the value calculated by Demoulin.[29] Leach et al.[12] assigned in their photophysical studies the broad continuum around 7.5 eV mainly as a diffuse Rydberg transition accompanied by an additional $\sigma_{CO} \rightarrow \pi^*$ valence transition mixing with the Rydberg state. They concluded this on the basis of estimated oscillator strength of $f \approx 0.025$. However, our calculations do not support this assignment: no mixing with a valence transition can be observed. As can be seen from Figure 2, the upper orbital 8a′ can be characterized as a 3s-Rydberg MO. The calculated oscillator strength of $f = 0.006$ for this state corresponds to values expected for a Rydberg transition. The value of 7.85 eV for the corresponding triplet state underlines together with the oscillator strength the genuine Rydberg character of this excitation. The finding that our calculation places the triplet state erroneously slightly (<0.07 eV) above the corresponding singlet state for this and two further Rydberg-type transitions above 8.0 eV emphasizes the small error margin of our present calculation.

Another Rydberg-type transition (7a′ → 9a′) originating from the HOMO is calculated at 8.44 eV (146.9 nm). The unexpectedly large oscillator strength of $f = 0.06$ can be understood from Figure 2: in the virtual MO 9a′, the p-AO located at O(2) is overlapping with the p-AO located at the carbon center, leading to a distorted asymmetric $\pi_{CO(2)}$-bonding. Bell et al.[16] and Leach et al.[12] place this Rydberg transition in their experimental work at 8.95 and 8.84 eV, respectively; Demoulin[29] calculated a value of 9.16 eV.

The third Rydberg transition (7a′ → 4a″) is calculated at 8.99 eV (137.9 nm), again in good agreement with the experimental measurements of Bell et al.[16] and Ari et al.[15] and the calculations reported by Demoulin.[29] This transition from the HOMO into the strongly diffuse p-type Rydberg MO 4a″ is obtained with a small oscillator strength of $f = 0.0003$.

Below 9 eV, the spectrum of formic acid is dominated by the excitation 2a″ → 3a″ (HOMO−1 into the LUMO). As can be seen from Table 1, our presently calculated 8.83 eV (140.4 nm) is somewhat larger than the experimental measurements of Fridh,[13] Ari et al.[15] (both 8.4 eV), and Leach et al.[12] (8.11 eV) but lower than the values reported from all other prior calculations. This valence transition corresponds to a $\pi_{C=O(1)} \rightarrow \pi^*$ excitation: as can be seen from Figure 2, the 2a″ MO consists mainly of the out-of-plane π bond of the carbonyl group and the lone pair located at the oxygen of the OH-group, whereas the 3a″ MO is antibonding (π^*-type O═C−O). The calculated oscillator strength of $f = 0.2$ is typical for this type of valence transition and agrees well with the measurements of Leach et al.[12] who report approximately the same value. The presently computed singlet−triplet splitting of 2.3 eV underlines the strong valence character of this transition.

3.2. The Spectrum of Chloroformic Acid. Table 2 summarizes the computed electronic spectrum of chloroformic acid up to 9.5 eV. The ground state of the molecule is a singlet state X^1A' with the electronic configuration $(9a')^2(3a'')^2$; again only valence electrons are stated. Because of the larger number of electrons to be treated active in the MRD-CI calculations, the more economic cc-pVDZ+SPD basis is used. This is justified because the use of this basis set resulted in reasonable values for the electronic spectrum of formic acid as can be seen from Table 1, in which we compare our computed values with both experimental measurements and prior calculations of HCOOH.

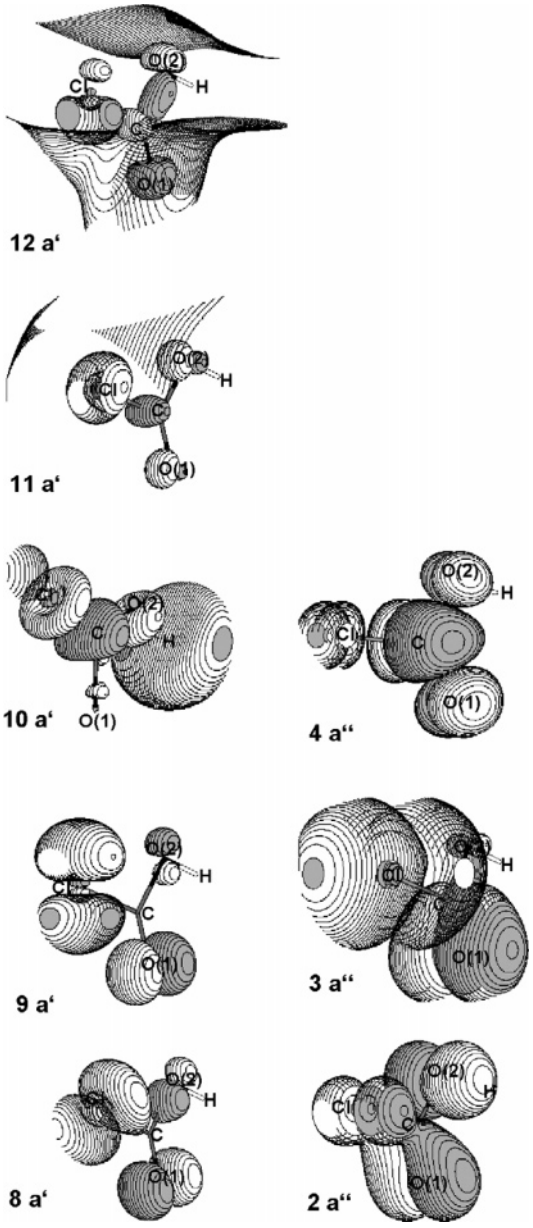

Figure 3. Charge density contours of characteristic occupied (8a′, 9a′, 2a″, and 3a″) and virtual orbitals (4a″, 10a′, 11a′, and 12a′) of chloroformic acid ClCOOH.

To test the importance of including Rydberg functions in the basis set, we furthermore performed calculations with a pure cc-pVDZ basis set without augmentation of Rydberg functions. Contrary to formic acid, the results listed in Table 2 show that there are only minor differences for excitation energies and oscillator strengths between cc-pVDZ and cc-pVDZ+SPD calculations up to 8.5 eV. This indicates that excitations in the spectrum of chloroformic acid up to 8.5 eV are mainly valence-type transitions, an assumption that is also supported by the remarkable singlet−triplet splittings. For the electronic spectrum of ClCOOH, one can expect to find transitions involving the carbonyl group and the O═C−O framework similar to formic acid. Furthermore, additional transitions are expected due to the substitution of hydrogen with chlorine.

The energetic ordering of the MOs of ClCOOH is ...$(5a')^2$-$(6a')^2(7a')^2(2a'')^2(8a')^2(3a'')^2(9a')^2$. As a result of the existence of the chlorine in the molecule, the spectrum becomes more

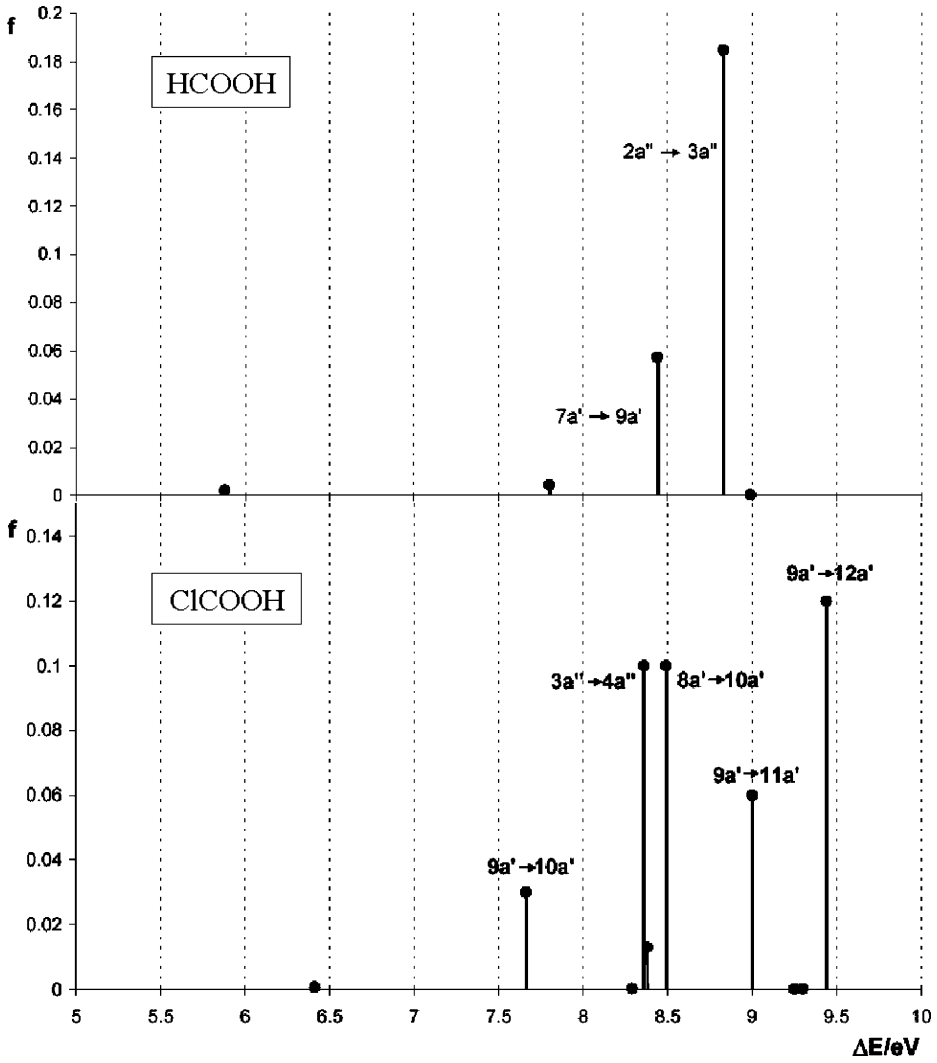

Figure 4. A comparison of the calculated electronic spectrum of formic acid HCOOH and chloroformic acid ClCOOH.

complex as compared to HCOOH, and excitations not only from the highest occupied molecular orbital HOMO 9a′ and the valence orbital 3a″ but also from the outer valence orbitals 8a′ and 2a″ into the low-lying virtual orbitals 4a″ (LUMO), 10a′, 11a′, and 12a′ can be expected to be low-lying. In Figure 3, we present charge density contours of important occupied (8a′, 9a′, 3a″, and 2a″) and virtual (4a″, 10a′, 11a′, and 12a′) molecular orbitals of ClCOOH.

Our calculation places the lowest energy singlet transition (HOMO−LUMO) 9a′ → 4a″ at 6.41 eV (193.4 nm), about 0.5 eV higher than the corresponding HOMO−LUMO transition of formic acid. As can be seen from Figure 3, this excitation corresponds to a $n_{Cl} \rightarrow \pi^*_{(C-Cl)}$ mixed with a $n_{O(1)} \rightarrow \pi^*_{OCO}$ and $n_{O(2)} \rightarrow \pi^*_{OCO}$-type transition within the O═C−O framework. The location of the AO contributions of chlorine and both oxygen centers in the LUMO is perpendicular to their alignment in the HOMO. Consequently, this transition is a weak one with a calculated oscillator strength of $f = 0.0007$ similar to the lowest-lying transition of formic acid.

The second low-lying transition is computed at 7.66 eV (161.9 nm) with an oscillator strength of $f = 0.03$. As can be seen from Figure 3, this 9a′ → 10a′ excitation is also valence type, in line with a singlet−triplet splitting of 0.35 eV. It can be characterized as a $n_{Cl} \rightarrow \sigma^*_{(C-Cl)}$ and a $n_{O(2)} \rightarrow \sigma^*_{(OH)}$-type transition. The antibonding character between carbon and chlorine of the LUMO+1 combined with the oscillator strength of $f = 0.03$ indicates that this excited state is repulsive for C−Cl splitting, leading to a dissociation of chloroformic acid. Because this transition is dominated by the $n_{Cl} \rightarrow \sigma^*_{(C-Cl)}$, there is no analogue in the spectrum of formic acid.

The excited $3^1A'$ state is computed at 8.36 eV (148.3 nm) and corresponds to the strong $\pi_{(C=O)} \rightarrow \pi^*_{(C=O)}$ transition. For the similar excitation in the electronic spectrum of formic acid, both Fridh[13] and Ari et al.[15] measured 8.4 eV. The calculated oscillator strength of $f = 0.1$ as well as the singlet−triplet splitting of 0.4 eV meet the expected values for this kind of valence transition.

The following excitation 3a″ (HOMO−1) → 10a′ (LUMO+1) is calculated at 8.29 eV (149.6 nm) erroneously 0.07 eV below 3a″ → 4a″ (LUMO). This small difference might serve as an indication for the error margin of the present calculation, which is well below 0.3 eV. Despite this small error margin of the present calculation, future experimental measurements might result in a larger energy range due to the broadness of this peak, which is known for the corresponding transition of formic acid. This 3a″ → 10a′ transition corresponds to a $n_{Cl} \rightarrow \sigma^*_{(C-Cl)}$-type excitation and possesses a rather weak oscillator strength of $f = 0.0003$, which can be understood from Figure 3, because the MOs 3a″ and 10a′ fall into perpendicular planes.

The HOMO−2 8a′, which is involved in the following transitions, consists of lone pairs located at the chlorine (n_{Cl}) and both oxygen centers ($n_{O(1)}$ and $n_{O(2)}$). The lone pairs n_{Cl} and $n_{O(2)}$ in the 8a′ MO are of p_z character, whereas those in the HOMO 9a′ are of p_y character. The excitations into the

LUMO 4a″ ($n_{Cl} \rightarrow \pi^*_{(C-Cl)}$) at 8.38 eV (148.0 nm) and the LUMO+1 10a′ ($n_{Cl} \rightarrow \sigma^*_{(C-Cl)}$) at 8.49 eV (146.0 nm) are somewhat stronger than the corresponding transitions out of the HOMO 9a′. Additionally, a $n_{(O2)} \rightarrow \sigma^*_{(O-H)}$ transition contributes to the 8a′ → 10a′ excitation, leading together with the $n_{Cl} \rightarrow \sigma^*_{(C-Cl)}$ system to an calculated oscillator strength of $f = 0.1$.

A further valence transition is computed at 9.25 eV (134.0 nm) with a weak oscillator strength of $f = 0.0002$. This 2a″ → 10a′ excitation can be characterized as a $\pi_{(C-Cl)} \rightarrow \sigma^*_{(C-Cl)}$ transition as can be seen from Figure 3.

Excitations into higher virtual orbitals, that is, 11a′ and 12a′, can be assigned as Rydberg-type transitions. The 9a′ → 11a′ excitation calculated at 9.00 eV (137.8 nm) can be characterized as originating from the n_{Cl}, $n_{O(1)}$, and $n_{O(2)}$ AO contributions of the HOMO 9a′ into the s-type Rydberg MO 11a′ (see Figure 3). A similar s-type Rydberg transition of formic acid is computed at 7.80 eV. The rather large oscillator strength of $f = 0.06$ is caused by a multireference nature of this excited state: besides 9a′ → 11a′ ($c^2 = 0.42$), also the strong valence transition 8a′ → 10a′ contributes remarkably ($c^2 = 0.11$). The same is found for the second Rydberg-type transition originating from the HOMO, which is calculated at 9.44 eV (131.2 nm). A mixing of the leading configuration 9a′ → 12a′ (Rydberg-type) with the valence excitations 8a′ → 10a′ and 3a″ → 4a″ leads to an oscillator strength of $f = 0.12$. As can be seen from Figure 3, the transition 9a′ → 12a′ can be characterized as an excitation from the n_{Cl} in the HOMO into a p-type Rydberg MO 12a′.

The second excitation into the s-type Rydberg MO 11a′ is originating from the HOMO−1 (3a″). Its value is calculated at 9.30 eV (133.3 nm) energetically close to the valence state 4 A″. A strong mixing of the configuration of this valence state (4 A″) with the configuration of the Rydberg transition (3a″ → 11a′) causes the large singlet−triplet splitting of almost 0.5 eV.

An important $\pi \rightarrow \pi^*$-type transition is computed at 8.98 eV (138.1 nm) employing the smaller cc-pVDZ basis set without Rydberg functions. Its large oscillator strength of $f = 0.28$ can be understood because this excitation can be characterized as $\pi_{(C-Cl)} \rightarrow \pi^*_{(C-Cl)}$ and $\pi_{(C=O)} \rightarrow \pi^*_{(C=O)}$ type (see Figure 3). Because of the large number of Rydberg states in the energy range around 9 eV, this $\pi \rightarrow \pi^*$-type excitation is not selected within the lowest 8 roots when employing the cc-pVDZ+SPD basis set. The corresponding triplet state is selected because it is calculated rather low in energy at 6.85 eV. Again, this large singlet−triplet splitting underlines the valence nature of this state. Leach et al.[12] assigned the corresponding $\pi_{(C=O)} \rightarrow \pi^*$ transition in the experimental electronic spectrum of formic acid at 8.92 eV.

Figure 4 shows a sketch to compare the calculated electronic absorption spectra of formic acid and chloroformic acid. The electronic spectrum of formic acid is dominated by a valence transition at 8.8 eV (140 nm) (2a″ → 3a″) and the Rydberg-type transition (7a′ → 9a′) at 8.4 eV (147 nm). As can be seen, the spectrum of chloroformic acid is more complex. As a consequence, the best possibility to differentiate between the two acids by important transitions in their electronic absorption spectra is to look at the energy window below 8 eV (155 nm), because there can be observed only a weak absorption band of formic acid originating from Rydberg transitions, whereas a strong valence-type excitation can be expected in the spectrum of chloroformic acid at 7.7 eV (161 nm). Further important transitions in the spectrum of chloroformic acid are predicted at 8.4 (148 nm), 8.5 (146 nm), 9.0 (138 nm), and 9.4 eV (131 nm). In a mixture of both acids, these states of ClCOOH probably will be difficult to differentiate from transitions in the spectrum of formic acid because published spectra of formic acid[12,13,23] are known to be quite complex above 8 eV due to the considerable number of Rydberg-type transitions.

4. Summary and Conclusions

We employed multireference configuration interaction (MRD-CI) calculations to compute the electronic spectra of chloroformic and formic acid. Our results presently obtained for formic acid are in reasonable agreement with prior calculations[13,14,27−29] and experimental measurements.[12,13,15,16,22] Below 9 eV, we confirm two valence-type transitions: the first one is the lowest energy singlet−singlet transition (HOMO−LUMO) 7a′ → 3a″ presently computed at 5.88 eV (210.9 nm), while the second is 2a″ → 3a″ (HOMO−1 into the LUMO) calculated at 8.83 eV (140.4 nm). These excitations correspond to $n_{O(1,2)} \rightarrow \pi^*_{OCO}$ and $\pi_{C=O(1)} \rightarrow \pi^*$, respectively, in line with *f*-values of 0.002 and 0.2.

The substitution of hydrogen by chlorine leads to additional electronic transitions in the yet to be observed spectrum of ClCOOH. The lowest energy singlet transition (HOMO−LUMO) is calculated at 6.41 eV (193.4 nm), about 0.5 eV higher than the corresponding HOMO−LUMO transition of formic acid. Besides $n_{O(1,2)} \rightarrow \pi^*_{OCO}$, this excitation corresponds to a $n_{Cl} \rightarrow \pi^*_{(C-Cl)}$. Further valence-type transitions are computed at 7.66 eV (161.9 nm; $n_{Cl} \rightarrow \sigma^*_{(C-Cl)}$ and $n_{O(2)} \rightarrow \sigma^*_{(OH)}$), 8.29 eV (149.6 nm, $n_{Cl} \rightarrow \sigma^*_{(C-Cl)}$), 8.36 eV (148.3 nm, $\pi \rightarrow \pi^*_{(C=O)}$), 8.38 eV (148.0 nm, $n_{Cl} \rightarrow \pi^*_{(C-Cl)}$), 8.49 eV (146.0 nm, $n_{Cl} \rightarrow \sigma^*_{(C-Cl)}$), and 9.25 eV (134.0, $\pi \rightarrow \sigma^*_{(C-Cl)}$). The $\pi \rightarrow \pi^*_{(C-Cl,\ C=O)}$ excitation is computed around 8.98 eV (138.1 nm). In the energy rage between 9 and 9.5 eV, we obtain a number of states, 5 A′ (9.0 eV), 6 A′ (9.3 eV), and 8 A′ (9.44 eV), with a mixing of Rydberg and valence character.

Considering a mixture of both acids, the states of ClCOOH above 8 eV (155 nm) will probably be difficult to differentiate from transitions in the spectrum of formic acid. Consequently, the best possibility to differentiate between the two acids by important transitions in their electronic absorption spectra is to look at the energy window below 8 eV (155 nm). In this energy range, there can be observed only a weak absorption band of formic acid originating from Rydberg transitions, whereas a strong valence-type excitation is predicted in the spectrum of chloroformic acid at 7.7 eV (161 nm).

Acknowledgment. M.G.-S. acknowledges a grant from the Research Council of Norway through the cultural exchange program between Norway and Austria. Sigrid D. Peyerimhoff is thanked for providing us with a version of the DIESEL-MRD-CI at Innsbruck. In addition, we want to thank Michael Hanrath for various improvements of the DIESEL program package. Basis sets were obtained from the Extensible Computational Chemistry Environment Basis Set Database, Version 11/29/01, as developed and distributed by the Molecular Science Computing Facility, Environmental and Molecular Sciences Laboratory, which is part of the Pacific Northwest Laboratory, P.O. Box 999, Richland, WA 99352, and funded by the U.S. Department of Energy.

References and Notes

(1) Crutzen, P. J.; Müller, R.; Brühl, C.; Peter, T. *Geophys. Res. Lett.* **1992**, *19*, 1113.

(2) Beukes, J. A.; D'Anna, B.; Bakken, V.; Nielsen, C. J. *Phys. Chem. Chem. Phys.* **2000**, *2*, 4049.

(3) Enghoff, M. B.; Von Hessberg, P.; Nielsen, C. J.; Johnson, M. S. *J. Phys. Chem. A* **2003**, *107*, 7667.

(4) Gola, A. A.; D'Anna, B.; Feilberg, K. L.; Sellevag, S. R.; Bache-Andreassen, L.; Nielsen, C. J. *Atmos. Chem. Phys. Discuss.* **2005**, *5*, 1.
(5) Lugez, C.; Schriver, A.; Schriver-Mazzuoli, L.; Lasson, E.; Nielsen, C. J. *J. Phys. Chem.* **1993**, *97*, 11617.
(6) Oyaro, N.; Sellevag, S. R.; Nielsen, C. J. *Environ. Sci. Technol.* **2004**, *38*, 5567.
(7) Sellevag, S. R.; Nielsen, C. J. *Asian Chem. Lett.* **2003**, *7*, 15.
(8) Mühlhäuser, M.; Schnell, M.; Peyerimhoff, S. D. *Mol. Phys.* **2002**, *100*, 2719.
(9) Mühlhäuser, M.; Schnell, M.; Peyerimhoff, S. D. *Mol. Phys.* **2002**, *100*, 509.
(10) Schnell, M.; Mühlhäuser, M.; Lesar, A.; Peyerimhoff, S. D. *J. Phys. Chem. A* **2003**, *107*, 6489.
(11) Li, Y.; Francisco, J. S. *J. Chem. Phys.* **1999**, *111*, 8384.
(12) Leach, S.; Schwell, M.; Dulieu, F.; Chotin, J.-L.; Jochims, H.-W.; Baumgärtel, H. *Phys. Chem. Chem. Phys.* **2002**, *4*, 5025.
(13) Fridh, C. *J. Chem. Soc., Faraday Trans. 2* **1978**, *74*, 190.
(14) Basch, H.; Robin, M. B.; Kuebler, N. A. *J. Chem. Phys.* **1968**, *49*, 5007.
(15) Ari, T.; Güven, M. H. *J. Electron Spectrosc. Relat. Phenom.* **2000**, *106*, 29.
(16) Bell, S.; Ng, T. L.; Walsh, A. D. *J. Chem. Soc., Faraday Trans. 2* **1975**, *71*, 393.
(17) Leach, S.; Schwell, M.; Talbi, D.; Berthier, G.; Hottmann, K.; Jochims, H.-W.; Baumgärtel, H. *Chem. Phys.* **2003**, *286*, 15.
(18) Ng, T. L.; Bell, S. *J. Mol. Spectrosc.* **1974**, *50*, 166.
(19) Barnes, E. E.; Simpson, W. T. *J. Chem. Phys.* **1962**, *84*, 2853.
(20) Price, W. C.; Evans, W. M. *Proc. R. Soc. London, Ser. A* **1937**, *162*, 110.
(21) Nagakura, S.; Kaya, K.; Tsubomura, H. *J. Mol. Spectrosc.* **1964**, *13*, 1.
(22) Ioannoni, F.; Moule, D. C.; Clouthier, D. J. *J. Phys. Chem.* **1990**, *94*, 2290.
(23) Suto, M.; Wang, X.; Lee, L. C. *J. Phys. Chem.* **1988**, *92*, 3764.
(24) Langford, S. R.; Batten, A. D.; Kono, M.; Ashfold, M. N. R. *J. Chem. Soc., Faraday Trans.* **1997**, *93*, 3757.
(25) Tabayashi, K.; Aoyama, J.-i.; Matsui, M.; Hino, T.; Saito, K. *J. Chem. Phys.* **1999**, *110*, 9547.
(26) Schwell, M.; Dulieu, F.; Jochims, H.-W.; Fillion, J.-H.; Lemaire, J.-L.; Baumgärtel, H.; Leach, S. *J. Phys. Chem. A* **2002**, *106*, 10908.
(27) Iwata, S.; Morokuma, K. *Theor. Chim. Acta* **1977**, *44*, 323.
(28) Peyerimhoff, S. D.; Buenker, R. J. *J. Chem. Phys.* **1969**, *50*, 1846.
(29) Demoulin, D. *Chem. Phys.* **1976**, *17*, 471.
(30) Dawson, G. A.; Farmer, J. C.; Moyers, J. L. *Geophys. Res. Lett.* **1980**, *7*, 725.
(31) Goldman, A.; Murcray, F. H.; Murcray, D. G.; Rinsland, C. P. *Geophys. Res. Lett.* **1984**, *11*, 307.
(32) Galloway, J. N.; Linkins, G. E.; Keene, W. C.; Miller, J. M. *J. Geophys. Res., [Atmos.]* **1982**, *87*, 8771.
(33) Keene, W. C.; Galloway, J. N. *J. Geophys. Res., [Atmos.]* **1986**, *91*, 466.
(34) West, H. L.; Rollefson, G. K. *J. Am. Chem. Soc.* **1936**, *58*, 2140.
(35) Pimentel, G. C.; Herr, K. C. *J. Chim. Phys. Phys.-Chim. Biol.* **1964**, *61*, 1509.
(36) Herr, K. C.; Pimentel, G. C. *Appl. Opt.* **1965**, *4*, 25.
(37) Jensen, R. J.; Pimentel, G. C. *J. Phys. Chem.* **1967**, *71*, 1803.
(38) Francisco, J. S.; Ghoul, W. A. *Chem. Phys.* **1991**, *157*, 89.
(39) Stephenson, E. H.; Smyk, B.; Macdonald, J. N. *J. Chem. Soc., Faraday Trans.* **1995**, *91*, 789.
(40) Davis, R. W.; Robiette, A. G.; Gerry, M. C. L.; Bjarnov, E.; Winnewisser, G. *J. Mol. Spectrosc.* **1980**, *81*, 93.
(41) Remko, M. *J. Mol. Struct.* **1999**, *492*, 203.
(42) Treutler, O.; Ahlrichs, R. *J. Chem. Phys.* **1995**, *102*, 346.
(43) TURBOMOLE has been designed by the Quantum Chemistry Group, U. o. K., since 1988. See, for example: Ahlrichs, R.; Bär, M.; Häser, M.; Horn, H.; Kölmel, C. *Chem. Phys. Lett.* **1989**, *162*, 165. Ahlrichs, R.; van Arnim, M. In *Methods and Techniques in Computational Chemistry: MOTECC-95*; Clementi, E., Corongiu, G., Eds; STEF: Cagliari, Italy, 1995.
(44) Woon, D. E.; Dunning, T. H., Jr. *J. Chem. Phys.* **1993**, *98*, 1358.
(45) Dunning, T. H., Jr.; Harrison, P. J. *Modern Theoretical Chemistry*; Plenum Press: New York, 1977; Vol. 2.
(46) Dunning, T. H., Jr. *J. Chem. Phys.* **1989**, *90*, 1007.
(47) Hanrath, M.; Engels, B. *Chem. Phys.* **1997**, *225*, 197.
(48) Buenker, R. J.; Peyerimhoff, S. D. *Theor. Chim. Acta* **1974**, *35*, 33.
(49) Buenker, R. J.; Peyerimhoff, S. D. *Theor. Chim. Acta* **1975**, *39*, 217.
(50) Ditchfield, R.; Del Bene, J. E.; Pople, J. A. *J. Am. Chem. Soc.* **1972**, *94*, 703.